Swiss J Palaeontol (2011) 130:277–296
DOI 10.1007/s13358-011-0024-5

On the osteology of *Tapejara wellnhoferi* KELLNER 1989 and the first occurrence of a multiple specimen assemblage from the Santana Formation, Araripe Basin, NE-Brazil

Kristina Eck · Ross A. Elgin · Eberhard Frey

Received: 28 May 2011 / Accepted: 9 August 2011 / Published online: 26 August 2011
© Akademie der Naturwissenschaften Schweiz (SCNAT) 2011

Abstract The postcranial elements of two similar sized and juvenile individuals, along with a partial skull, are attributed to the Early Cretaceous pterosaur *Tapejara wellnhoferi*. The remains, recovered from a single concretion of the Romualdo Member, Santana Formation, NE-Brazil, represent the first account of multiple specimens having settled together and allow for a complete review of postcranial osteology in tapejarid pterosaurs. A comparison of long bone morphometrics indicates that all specimens attributed to the Tapejaridae for which these elements are known (i.e. *Huaxiapterus*, *Sinopterus*, *Tapejara*) display similar bivariate ratios, suggesting that Chinese and Brazilian taxa must have exhibited similar growth patterns. An unusual pneumatic configuration, whereby the humerus is pierced by both dorsally and ventrally located foramina, is observed within *T. wellnhoferi*, while the pneumatic system is inferred to have invaded the hindlimbs via the femur in all members of the Azhdarchoidea. The partial preservation of the endocranial cavity allows for a reconstruction of the tapejarid brain, where despite a small orbit with respect to skull size, the presence of large flocculi and ocular lobes indicate that *Tapejara* possessed both excellent balancing and visual systems as a consequence of its aerial lifestyle.

Keywords Brazil · Lower Cretaceous · Santana Formation · Pterosauria · Tapejaridae · Osteology

Abbreviations

BSP	Bayerische Staatammlung für Paläontologie und historische Geologie, Munich, Germany
D	Dalian Natural History Museum, Dalian, China
IMNH	Iwaki City Museum of Coal and Fossils, Iwaki, Japan
IVPP	Institute for Vertebrate Palaeontology and Palaeoanthropology Beijing, P. R. China
MCT	Palaeontology section of the Department Nacional da Produção (Museu de Ciências da Terra), Rio de Janeiro, Brazil
MN	Museu Nacional, Rio de Janeiro, Brazil
NSM	National Science Museum, Tokyo, Japan
SMNK	Staatliches Museum für Naturkunde Karlsruhe, Karlsruhe, Germany
UOSG	Collection of Urs Oberli, St Gallen, Switzerland
ZMNH	Zhejiang Museum of Natural History, Hangzhou, China

Introduction

The Romualdo Member of the Santana Formation NE-Brazil is comprised primarily of a series of highly fossiliferous silts and shales, representing the deposits laid down as part as an extensive Archapelago setting during the latest part of the Early Cretaceous (Albian, e.g. Pons et al. 1990, 1996).

Electronic supplementary material The online version of this article (doi:10.1007/s13358-011-0024-5) contains supplementary material, which is available to authorized users.

K. Eck (✉)
Department of Geological Sciences, University of Heidelberg, 69120 Heidelberg, Germany
e-mail: kristina.eck@geow.uni-heidelberg.de

R. A. Elgin · E. Frey
Department of Geology, State Museum of Natural History Karlsruhe, 76133 Karlsruhe, Germany
e-mail: rosselgin@hotmail.com

E. Frey
e-mail: dinofrey@aol.com

Although the exact stratigraphical divisions of the region remain somewhat controversial (see Neumann and Cabrera 1999; Martill 2007 for discussion) the sequence is famous for its exceptional preservation of fish and other vertebrates, including dinosaurs and pterosaurs (e.g. Maisey 1991; Martill 2007; Unwin 1988; Wellnhofer 1991a), the bones of which acted as a nucleation point for carbonate precipitation after settling on the muddy floor. Fossils from these sediments are subsequently surrounded by a thick carbonate concretion that completely encases the bones of a single animal. With respects to pterosaurs, the Romualdo Member has provided many of the best and most influential pterosaurian specimens in recent years, however, the taxonomy of Santana ornithocheirids is famously confused and the taxonomic diversity itself has undoubtedly been inflated. To date, recovered specimens include the ornithocheiroids: *Araripesaurus castilhoi* (Price 1971), *Araripedactylus dehmi* (Wellnhofer 1977), *Anhanguera santanae* (Wellnhofer 1985, 1991a), *A. blittersdorffi* (Campos and Kellner 1985), *Brasileodactylus araripensis* (Kellner 1984), *Cearadactylus artox* (Leonardi and Borgomanero 1985), *C.? ligabuei* (Dalla Vecchia 1993), *Coloborhynchus robustus* (Fastnacht 2001), *C. spielbergi* (Veldmeijer 2003), *C. piscator* (Kellner and Tomida 2000), *Santanadactylus araripensis* (Wellnhofer 1985; Kellner and Tomida 2000), *Santanadactylus brasiliensis* (De Buisonjé 1980), *S. cf. pricei* (Wellnhofer 1985), *Ornithocheirus mesembrinus* (Wellnhofer 1987), and the azhdarchoids: *Tupuxuara longicristatus* (Kellner 1989), *T. leonardi* (Kellner and Campos 1994b), *T. deliradamus* (Witton 2009), *Thalassodromeus sethi* (Kellner and Campos 2002), *Tapejara wellnhoferi* (Kellner 1989; Wellnhofer and Kellner 1991).

The latter of these taxa, *T. wellnhoferi*, remains to date as one of the best represented of the Brazilian azhdarchoids, known from a collection of excellently preserved cranial material (AMNH 24440, UOSG 12891 Wellnhofer and Kellner 1991; MN 6595-V, Kellner 1989; MCT 1500-R Kellner 1996a, b). By contrast, published accounts of the postcranial skeleton are restricted to only a partial cervical series (i.e. AMNH 24440, Wellnhofer and Kellner 1991).

Herein we report on a partial skull and associated postcranial remains referred to the genus *T. wellnoferi*, the material providing the first complete overview of its osteology. Duplicate elements of differing size are observed within the postcranial skeleton, indicating the presence of at least two individuals (Fig. 1) and representing the first example of skeletal aggregation within pterosaur bearing concretions from the Romulado Member of the Santana Formation.

Preservation and identity

During preparation, a single concretion was found to contain the partial remains of a skull (premaxillomaxillary,

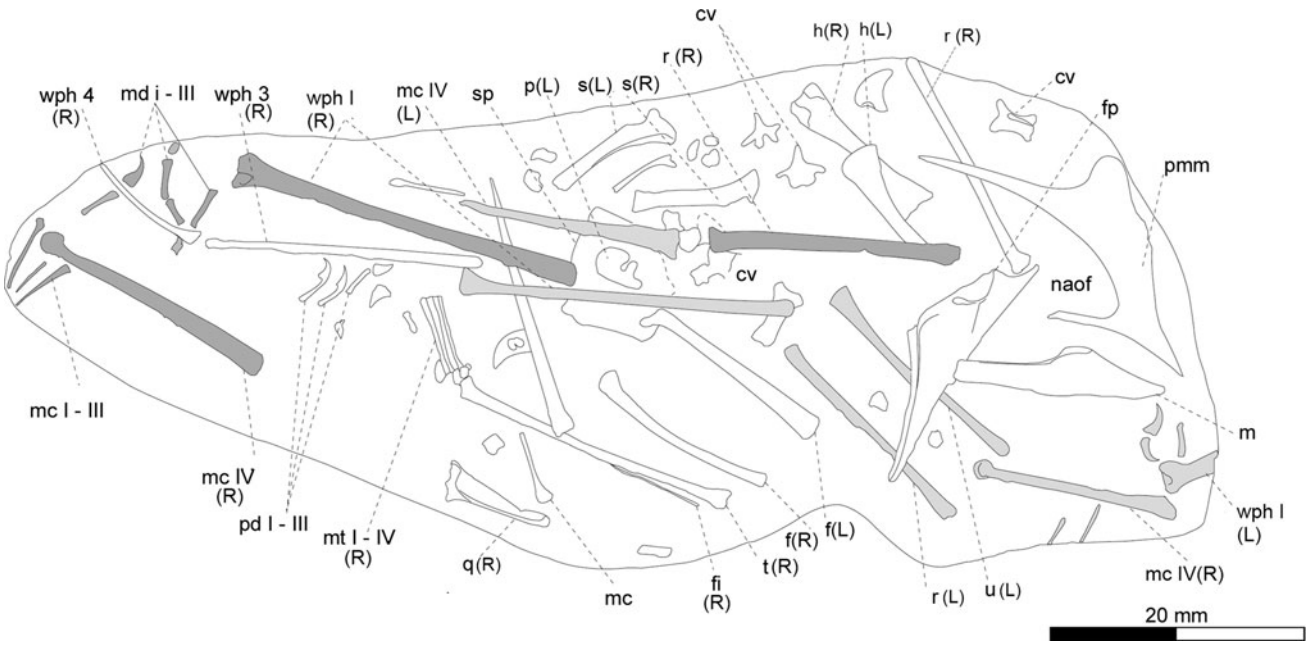

Fig. 1 Line drawing depicting the original position of skeletal elements of SMNK PAL 1137 prior to preparation. Elements attributed to the smaller Individual A are shaded in *light grey* while those belonging to the larger Individual B are shaded in *dark grey*. The remaining elements are tentatively attributed to Individual A, which preserves both wings along with the coracoid and sternal plate. *cv* cervical vertebrae, *f* femur, *fi* fibula, *fp* frontoparietal, *h* humerus, *m* mandible, *mc* metacarpal, *md* manual digits, *naof* nasoantorbital fenestra, *p* pubis, *pd* pedal digits, *pmm* premaxillomaxilla, *q* quadrate, *r* radius, *s* scapula, *sp* sternal plate, *t* tibia, *u* ulna, *wph* wing finger phalanx, (R) *right side*, (L) *left side*

mandible and neurocranium) and a variety of postcranial elements, including cervical, thoracic and caudal vertebrae, scapulae/coracoids, humeri, radii/ulnae, metacarpals, the first wing finger phalanges, elements of the ischiopubis and the complete hindlimbs. These elements were widely displaced about the concretion indicating that the carcasses were subject to a limited amount of disturbance after settling on the lagoon floor. The bones themselves are preserved in three dimensions and were fully extracted from the concretion. Due to the thinness of the sternum plate the dorsal face of the preserved bone was stabilised with epoxy resin during the preparation process. Only limited damage to the compacta is observed.

The presence of radii, metacarpals and wing finger phalanges of various sizes indicates the presence of at least two individuals. Although long bone elements of unequal length have been previously reported within single specimens (e.g. IVPP V-14377, Wang et al. 2008) and the physical lengths of the bones are similar, with the longer bones here being 1.3 times the size of the smaller elements, the longer elements are visually broader and more robust, and three first wing finger phalanges are known. Two of those phalanges are equal in size and represent the right and left wing fingers respectively, indicating that they came from a single individual. To prevent confusion the collection number SMNK PAL 1137 is used throughout this manuscript to collectively refer to all bones prepared from the original concretion, rather than to a specific individual, as is typical of other Santana fossils. Where necessary the smaller of the two individuals is referred to as "Individual A" and the larger of the two is "Individual B" (Table 1 in Electronic Supplementary Material).

Based on relative size and robustness, Individual A is represented by the sternum, right coracoid, radii, ulnae, wing metacarpals (Mc IV), and the first wing finger phalanges of the left and right wings. The larger Individual B is represented by the radius, fourth metacarpal and first wing finger phalanx of the left wing. The lack of any further comparable elements, along with the similarities in size and preservational state of the remaining bones, argues against the presence of any additional individuals. The similarities in overall size between the comparable elements of the two individuals however prevents the definite assignment of the remaining elements, which include the skull and mandible, cervical, thoracic and caudal vertebrae, the 2nd phalanx of the wing finger, the ilium, pubis, ischium, and prepubic bones, along with the femur, tibia and pes. As such, these are here noted as "miscellaneous elements," even though their association with one of the two specimens is not doubted (see discussion, Table 1 in ESM). The preservation of identical anatomical and pneumatic features on each of the duplicate elements leads the authors to conclude that both individuals are representative of the same genus. For the purpose of this description elements are described in unison, where in the case of duplicate bones, those showing the best preservation is preferentially described.

Systematic palaeontology

Order Pterosauria Kaup 1834
Suborder Pterodactyloidea Plieninger 1901
Superfamily Azhdarchoidea Unwin 1992
Family Tapejaridae Kellner 1989 (sensu Lü et al. 2006a)
Genus *Tapejara* Kellner 1989
Tapejara wellnhoferi Kellner 1989

Horizon and locality Exact locality unknown, but likely Sierra de Maosina due to the formerly blue colour of the original concretion. Romualdo Member, Santana Formation, Chapada do Araripe, Cerará, NE-Brazil. Lower Cretaceous (?Aptian/Albian).

Material Skull and associated postcranial elements collectively housed under the reference number SMNK PAL 1137.

Revised diagnosis As for *Tapejara wellnhoferi* (Kellner 1989 amended after Wellnhofer and Kellner 1991). In summary: edentulous azhdarchoid with short skull, high, median premaxillary sagittal crest occupying the rostral portion of the skull. Elongate frontoparietal crest present, extending posteriorly beyond the occipital plate. Very large nasoantorbital fenestra, orbit situated below the level of the dorsal margin of the nasoantorbital fenestra. Rostrum inclined ventrally with concave depression in palatal view, terminating in a pointed tip. Palate lacks a medial ridge. Median ventral crest present on the symphysis of the lower jaw. Occlusal margin of symphysis inclined ventrally with a concave depression along the dorsal face of the inclination. Cervical vertebrae with short, low neural spines and a pair of large pneumatic foramina lateral to the neural canal. The axis is lacking lateral pneumatic foramina. The presence of two pneumatic foramina piercing the humerus, one on the dorsal face of the bone at the base of the posterior process, and a second on the ventral face of the collum, is added to the generic diagnosis.

Description

Premaxillomaxilla

The maxilla, premaxilla, premaxillary crest and palatine that together form the rostral portion of the edentulous upper jaw, are fully co-ossified to form a single gracile unit with no trace of a dividing suture (Fig. 2; plate 1A). The

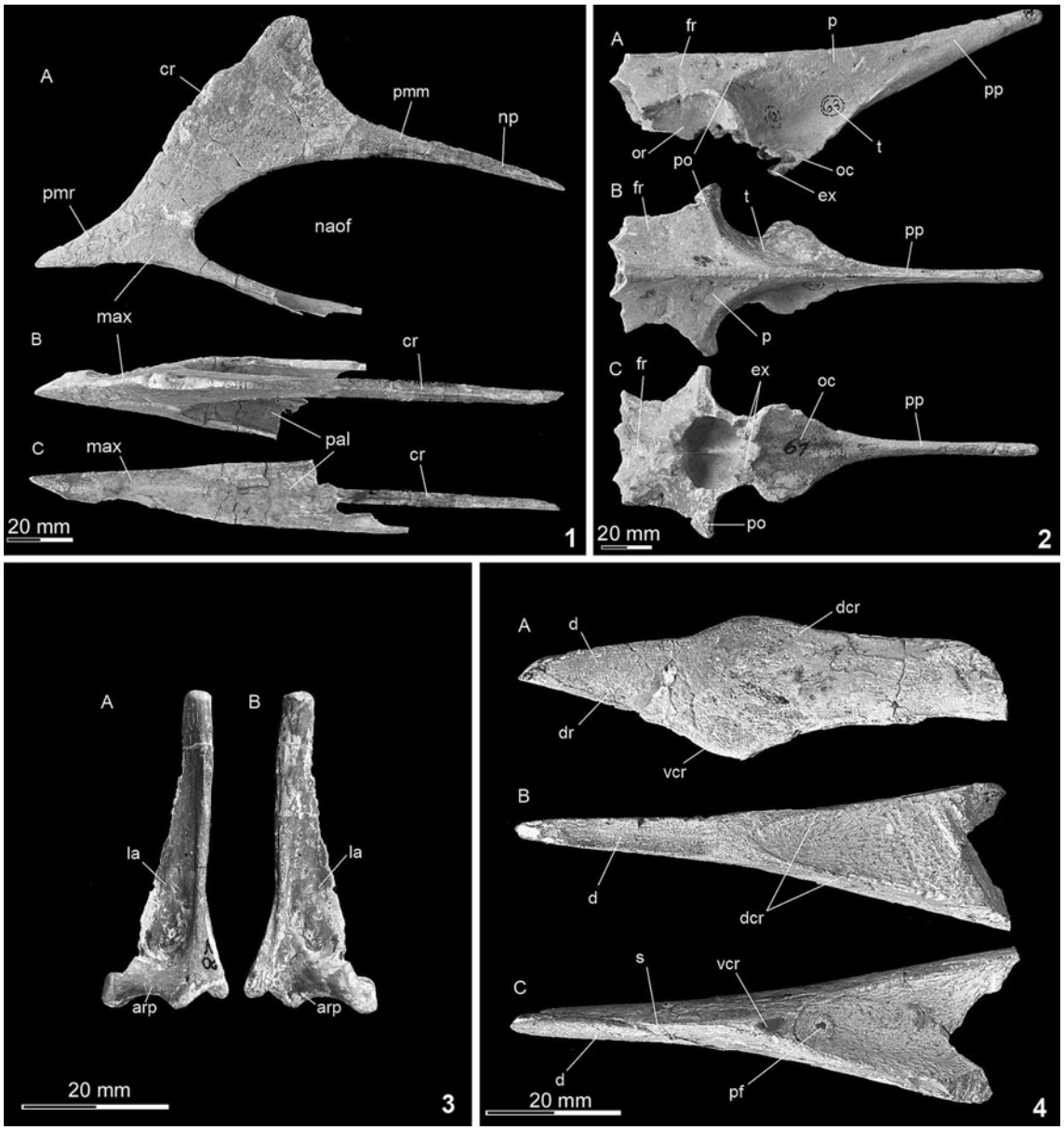

Fig. 2 Cranial elements of *Tapejara wellnhoferi*, SMNK PAL 1137. Plate **1**. Premaxillomaxilla in its *A* lateral, *B* dorsal, *C* ventral aspects. Plate **2**. Neurocranium in its *A* lateral, *B* dorsal, *C* ventral aspects. Plate **3**. Right quadrate in its *A* posterior, *B* anterior aspects. Plate **4**. Mandible in its *A* lateral, *B* dorsal, *C* ventral aspects. *arp* articular process, *cr* cranial crest, *d* dentary, *dcr* dorsal dentary crista, *dr* dentary rostrum, *ex* exoccipital process, *fr* frontal, *la* lamina, *max* maxilla, *naof* nasoantorbital fenestra, *np* nasal process, *oc* occipital, *or* orbit, *p* parietal, *pal* palatine, *pf* pneumatic foramen, *pmm* premaxillomaxilla, *pmr* premaxilla, *po* postorbital, *pp* parietal process, *vcr* ventral dentary crista

anterior margin of the rostrum is gently concave and merges dorsally into a high sagittal crest, the anterodorsal and dorsal portions of which are broken. On the lateral surface of the crest the compacta is partially eroded and fine trabeculae, orientated in a rostroventral-posteriodorsal direction, are observed. The rostrum is triangular in cross section, being at least four times as high as it is wide beneath the sagittal crest. The crest itself is comprised of two very thin blades of trabeculae braced bone, preserving a total cross sectional width of 2 mm towards its posterior margin.

The central region of the skull is dominated by the presence of a large, sub-oval nasoantorbital fenestra, terminating at a point 42.5 mm posterior to the anterior terminus of the rostrum. Its ventral and anteroventral margins are formed by the maxilla but have broken posteriorly before the inferred contact with the jugal. The dorsal roof of the fenestra is formed by the premaxilla, which extends

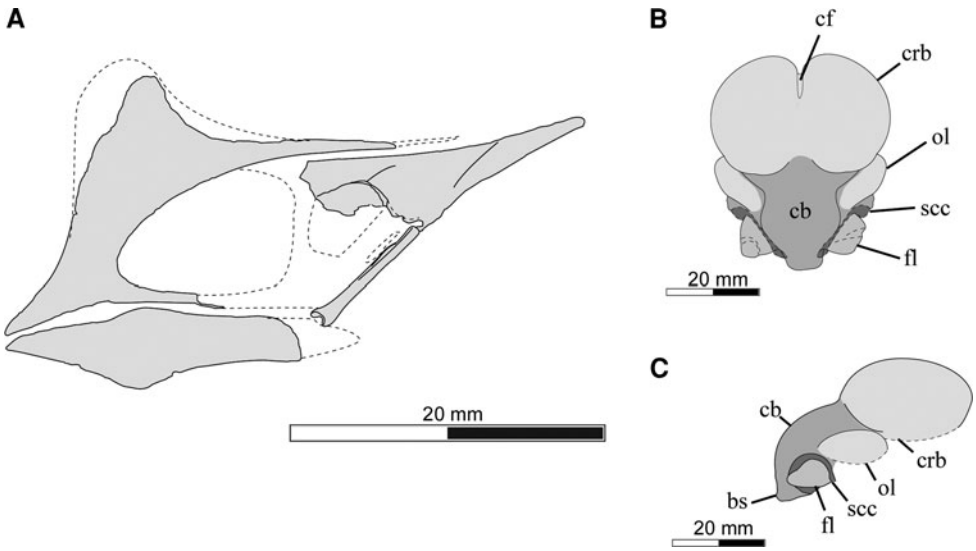

Fig. 3 *Tapejara wellnhoferi*, SMNK PAL 1133. **a** Reconstruction of the skull with preserved elements in grey. Endocranial cast of the described specimen, highlighting the details and lobes of the brain in dorsal (**b**) and right lateral views (**c**). *bs* brain stem, *cb* cerebellum, *cf* central furrow, *crb* cerebrum, *fl* floccular lobe, *ol* ocular lobe, *scc* semi-circular canals

posteriorly as a low, triangular strut, no more than 4 mm in thickness.

The palatines form the ventral floor of the nasoantorbital fenestra and are smooth and gently convex in transverse section, with a width of 14 mm immediately ventral to the anterior termination of the fenestra (Fig. 2; plate 1B, C). Anterior to the nasoantorbital fenestra the palate becomes transversely concave and tapers to a point at the tip of the skull.

Neurocranium

The frontal and parietal have fused together to form the posterodorsal roof of the skull, the preserved unit encompassing part of the occipital region (located dorsal to the foramen magnum), along with the dorsal margin of the orbit and a large portion of the endocranial cavity as seen from ventral view (Fig. 2; plate 2C). The frontals are transversely concave and have fully fused to form a high ridge along the median sagittal plane of the skull. The anterolateral, lateral and posterolateral margins of the bone are both concave in profile and respectively form the articular surfaces for the prefrontals and the dorsal rim of the orbit. The parietal forms part of the medial surface of the supratemporal fenestra, however, its true extent is unclear as all sutures of the neurocranial unit are closed. The likely contact between the anterior margin of the parietal and the posterior portion of the frontal appears to be a pronounced ridge that has developed off the posterodorsal rim of the orbit, separating the frontal from the anterior limit of insertion for the *m adductor mandibulae*. A prominent, blade-like parietooccipital process extends for 58 mm in a posterodorsal direction from the posterodorsal margin of the skull (Fig. 2; plate 2). The occipital region is very badly preserved but is gently concave and pierced by two laterally located foramina (Fig. 2; plate 2A). The dorsal roof of the foramen magnum is observed along the ventrally preserved margin of the bone.

Endocranial cavity

The neurocranial block has broken open ventrally to expose the endocranial cavity. A silicone cast of the cavity was made and forms the basis of this description (Fig. 3b, c). The mould so closely resembles the shape of a brain that, in contrast to other reptiles and in agreement with previous authors (Wellnhofer 1991b; Kellner 1996a, b; Bennett 2001), it is taken as an exact match of the pterosaurian brain.

The entire brain is directed dorsally at an angle of around 45° when the skull is orientated horizontally, the anterior portion being formed by the two large, bean-shaped lobes of the cerebrum. The lobes are transversely convex with regularly curved anterior margins and are separated from one another by a deep median sulcus that becomes very pronounced on the anterior half of the cerebrum. Immediately anterior to the endocranial cavity there is a small, reversed V-shaped opening into which the olfactory lobes would have been positioned. The size and shape of these lobes however cannot be determined. The cerebellum occupies the median portion of brain, immediately posterior to the cerebral lobes. It is smoothly convex in its dorsal aspect and can be traced as far ventrally as the dorsal margin of the foramen magnum, forming the top of the brain stem. The cerebellum is bordered on its anterolateral margins by the ocular lobes and by the osseous labyrinth along its posterolateral margin. Its dorsal surface displays a strong and regular concave curvature. Despite being incomplete and lacking their ventral portions, the occipital lobes and the osseous labyrinths are both very large. The thin walled, arch-like tube of the

osseous labyrinth is well defined, leaving a deep depression on the endocast around the floccular lobes. The preservation of a small portion of the lateral semicircular canal suggests that this structure would have completely surrounded the flocculus.

Quadrate

The right quadrate is complete but lies unfused to the other elements of the skull. The bone is formed by two branches, orientated dorsoventrally and mediolaterally, and connected by a thin diagonal laminae of bone to give the element an L-shaped appearance in its posterior aspect (Fig. 2; plate 3). The dorsoventrally directed branch is 2.4 times the length of the horizontal branch; the dorsal termination of the former being smooth and well rounded in posterior view and preserving an oval shaped cross section. The ventrolateral margin of the bone forms the articular facet for the mandible where a pronounced sulcus runs in an anteromedial direction. A left quadrate of a comparable size to that described above is also present in the concretion but the vertical branch is broken only just dorsal to its base.

Mandible

The mandible is edentulous and preserves a short symphysis only 44 mm in length, formed by the completely co-ossified contralateral rami. The dorsal face of the symphysis is transversely concave and is directed anteroventrally at an angle of 18°, starting at a point 45 mm posterior of the rostral tip (Fig. 2; plate 4B). The ventral margin is almost straight but forms a sagittal crest reaching its maximum depth at the symphysis. In its dorsal aspect the bone appears as an elongate triangle, three times as long as it is wide (Fig. 2; plate 4) while the posterior section containing the articular facet is missing.

Cervical vertebrae

Four procoelous vertebra, identified as elements of the cervical series, are observed in various states of preservation (Fig. 4). Two of these are attributed to the middle cervical column (Fig. 4f–o) while a third is identified as the 7th cervical. The remaining element represents the isolated axis (Fig. 4a–e).

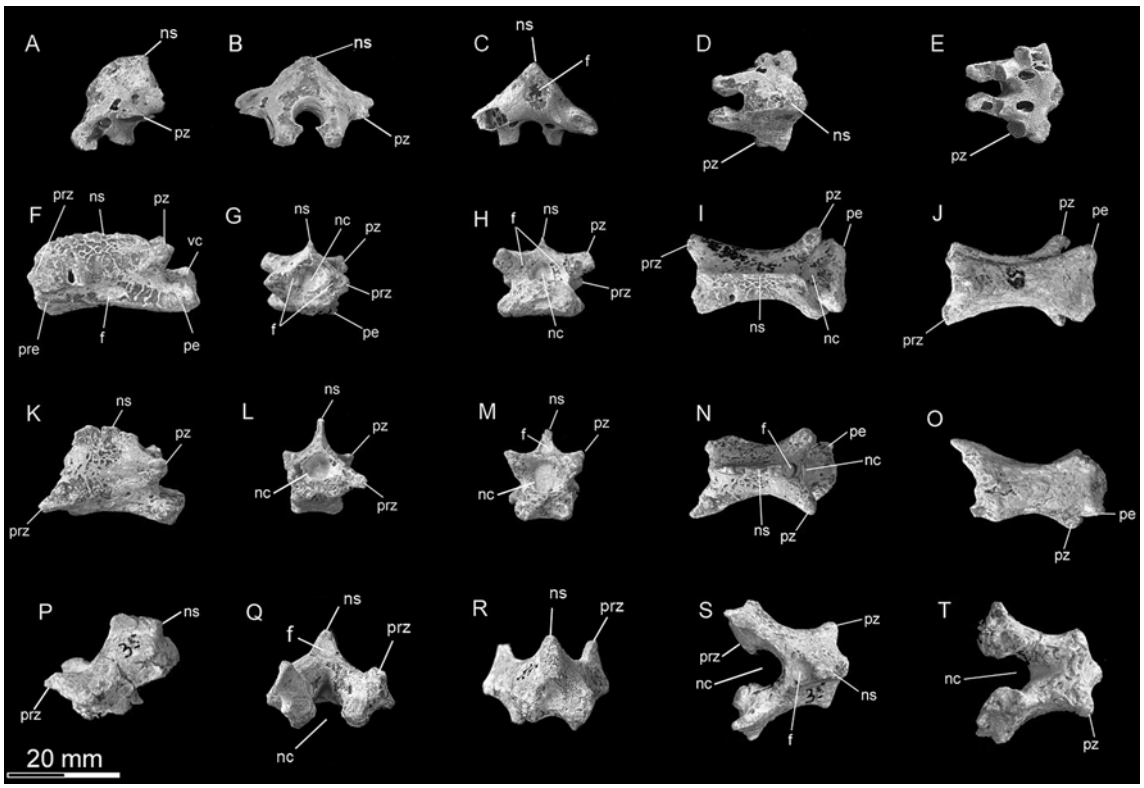

Fig. 4 Cervical elements of *Tapejara wellnhoferi*, SMNK PAL 1137, where: *A–E* axis in lateral (*A*), anterior (*B*), posterior (*C*), dorsal (*D*) and ventral view (*E*); *F–J* cervical vertebra in lateral (*F*), anterior (*G*), posterior (*H*), dorsal (*I*) and ventral view (*J*); *K–O*, cervical vertebra in lateral (*K*), anterior (*L*), posterior (*M*), dorsal (*N*) and ventral view (*O*); *P–T*, 7th cervical vertebra in lateral (*P*), anterior (*Q*), posterior (*R*), dorsal (*S*) and ventral view (*T*). *f* foramen, *nc* neural canal, *ns* neural spine, *pe* postexapophysis, *pre* preexapophysis, *pz* postzygapophysis, *prz* prezygapophysis, *vc* vertebral condyle

The complete neural arch of the axis is preserved but missing any trace of the atlas or the centrum. The neural arch itself is almost as long as it is wide. The prezygapophyses that flank the neural canal extend in an anterior direction, while the transverse processes that occupy the posterior half of the lateral face are directed laterally. The bone therefore has a sub-triangular profile in both its anterior and lateral aspects. The sub-triangular neural spine of the axis is orientated in a slightly posterodorsal direction but has broken only just above its base. The neural canal occupies the ventral half of the anterior face of the bone, positioned slightly dorsal to the prezygapophyses, and is almost circular with a diameter of 4 mm. Approximately halfway up the neural arch of the axis the postzygapophyses extend laterally for a short distance. The articular face is flat and rounded, with a diameter of 4 mm, and orientated parallel to the transverse plane. Immediately posterior to the postzygapophyses a posterolaterally directed lobe of bone has developed. The posteromedial face of this lobe is concave and rugose for the attachment of neck muscles. A large foramen pierces the bone on the lateral face, just anterior to the postzygapophyses, while on the posterior face of the axis, two foramina flank the dorsal half of the neural canal. In its ventral aspect four peduncles are arranged in a rectangular pattern for the articulation of the centrum (Fig. 4e).

The middle cervicals (Fig. 4f–o) are elongate elements, just over three times as long as they are wide at their narrowest point. A single foramen pierces the lateral face of the centrum of the more elongate element (Fig. 4f). The non-articular portions of the pre- and postzygapophyses are widely splayed, forming an angle of 27–44° with the sagittal plane in dorsal view. The neural spines are relative long compared to those more posterior vertebrae, however, the height differs substantially depending on the original position of the element within the cervical column. In one element (Fig. 4f–j) the neural spine, while broken, appears to have been very low and thin, while in another the neural spine is taller and more robust, at least half as tall as it is long. The posterior face of the latter is pierced by a single large foramen dorsal to the neural arch (Fig. 4m). The lateral faces of the neural spines are strongly concave. The anterior faces of the vertebrae are dominated by the neural canal, flanked on each side by a smaller, sub-circular foramen. In both vertebrae the postzygapophyses are positioned dorsal to the level of the prezygapophyses.

The posteriormost of the preserved cervicals (i.e. c7, Fig. 4p–t) is shorter, only 2/3rd as long as those of the middle cervical series, but is very different in form. The neural arch is short, producing a rectangular neural spine that would have been slightly taller than it was long. The anterior braches of the neural arch are large and splayed anterolaterally at an angle of 33° to the sagittal plane and are more robust than those of the preceding vertebrae. The centrum of the vertebrae is missing and the peduncles on the ventral face of the neural arch are badly damaged. A large foramen, located dorsal to the neural canal pierces the anterior face of the neural spine and exits onto its posterior surface.

Thoracic vertebrae

Four thoracic vertebrae are identified. In two of these elements the neurocentral sutures are completely closed while in the remaining two the centrum is missing, indicating that not all the elements of the thoracic column had reached their mature state (Fig. 5). A single vertebra (Fig. 5p–t) is small and light in construction relative to the other vertebrae, with gracile transverse processes, indicating a more posterior position within the thoracic vertebral series. The remaining three vertebrae are larger with large posterolaterally directed transverse processes, indicating an association with the middle or more anterior portion of the thoracic column. Aside from the inherent differences in size, the vertebrae are similar in morphology with short central bodies and neural arches, as well as dorsally orientated neural spines that display a rectangular profile in their lateral aspect. The posterior faces of the neural spines are high and triangular in outline, the centre of which is deeply depressed and pierced with foramina. The postzygapophyses are positioned on the ventrolateral margins of the neural arch. These lie dorsal to the level of the prezygapophyses, the flat articular surfaces orientated dorsolaterally in anterior view at an angle of 30° to the transverse plane. Differences between the vertebrae are observed in the number and position of foramina, where a large foramina pierces the lateral and anterolateral faces of the neural arch in one (Fig. 5p–t) but are absent in the remaining vertebrae. In two vertebrae (Fig. 5f–j, p–t) the foramina piercing the posterior face of the neural spine exit onto its anterior face.

Caudal vertebrae

Only a single, sub-rectangular and opisthocoelous centrum of the caudal series is preserved. The ventral surface of the vertebral body is transversely constricted. The dorsal margin is broken and it is impossible to determine whether the neural spine is missing due to the lack of ontogenetic fusion or taphonomic damage.

Rib

The proximal part of a small, double headed rib, containing costal head and neck and likely belonging to the more

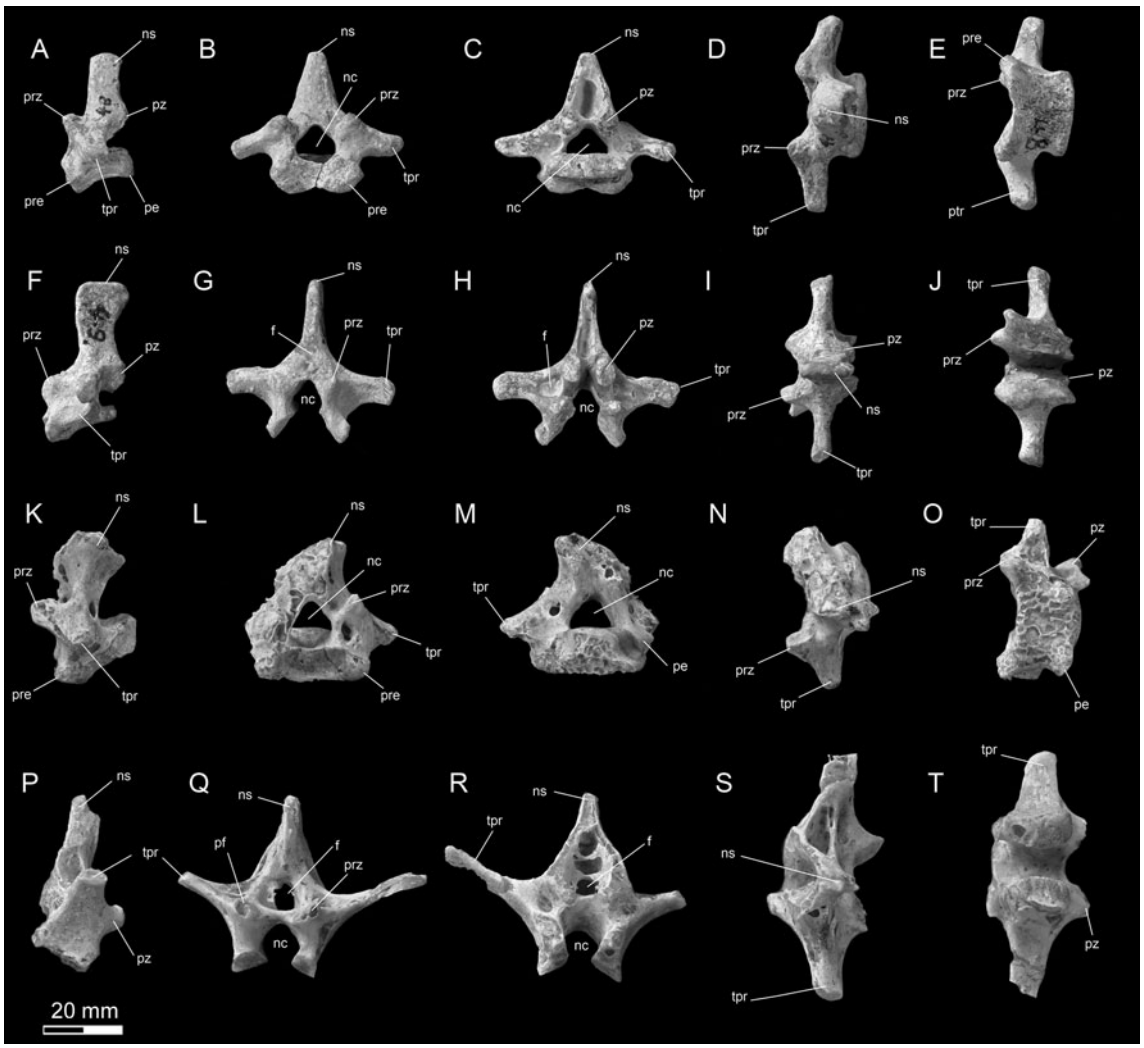

Fig. 5 *Tapejara wellnhoferi*, SMNK PAL 1137: Thoracic vertebrae. Four indeterminate thoracic vertebrae in their lateral (*A*, *f*, *K*, *B*), anterior (*B*, *G*, *I*, *Q*), posterior (*C*, *H*, *M*, *R*) dorsal (*D*, *I*, *N*, *S*), and ventral (*E*, *J*, *O*, *T*) aspects. *f* foramen, *nc* neural canal, *ns* neural spine, *pe* postexapophysis, *pre* preeyapophysis, *prz* prezygapophysis, *pz* postzygapophysis

posterior portion of the thoracic series, is preserved. Only the proximal part with costal head and neck is preserved, where the capitulum forms as an elongate process that terminates in a half-rounded, but fractured surface.

Sternum

In its dorsal aspect the sternal plate is sub-rectangular but strongly concave in its transverse section, resulting in the lateral margins of the plate being positioned dorsal to the level of the cristospine (Fig. 6; plate 1B). A series of crenulations observed along the left lateral margin of the sternal plate are interpreted as the articular facets for the anterior sternocostae. A single large foramen (7 mm in diameter) pierces the dorsal surface of the plate immediately posterior to the sternal neck, defined by where the anterior margins of the plate contact the cristospine (Fig. 6; plate 1B). The cristospine is short, forming 18% the total length of the sternal, and has been damaged such that the sternocoracoid articulations are badly worn and very faint (Fig. 6; plate 1A, B). The ventral margin of the cristospine extends onto the ventral surface of the sternal plate for a distance of 9 mm, forming a very low and blunt ridge.

Coracoid

The coracoid blade is complete and offset against the remains of the coracoideal body at an angle of 134° (Fig. 6; plate 2). The blade is very narrow medial to the body but the posterior margin expands in a posterior direction approaching the medial termination of the bone

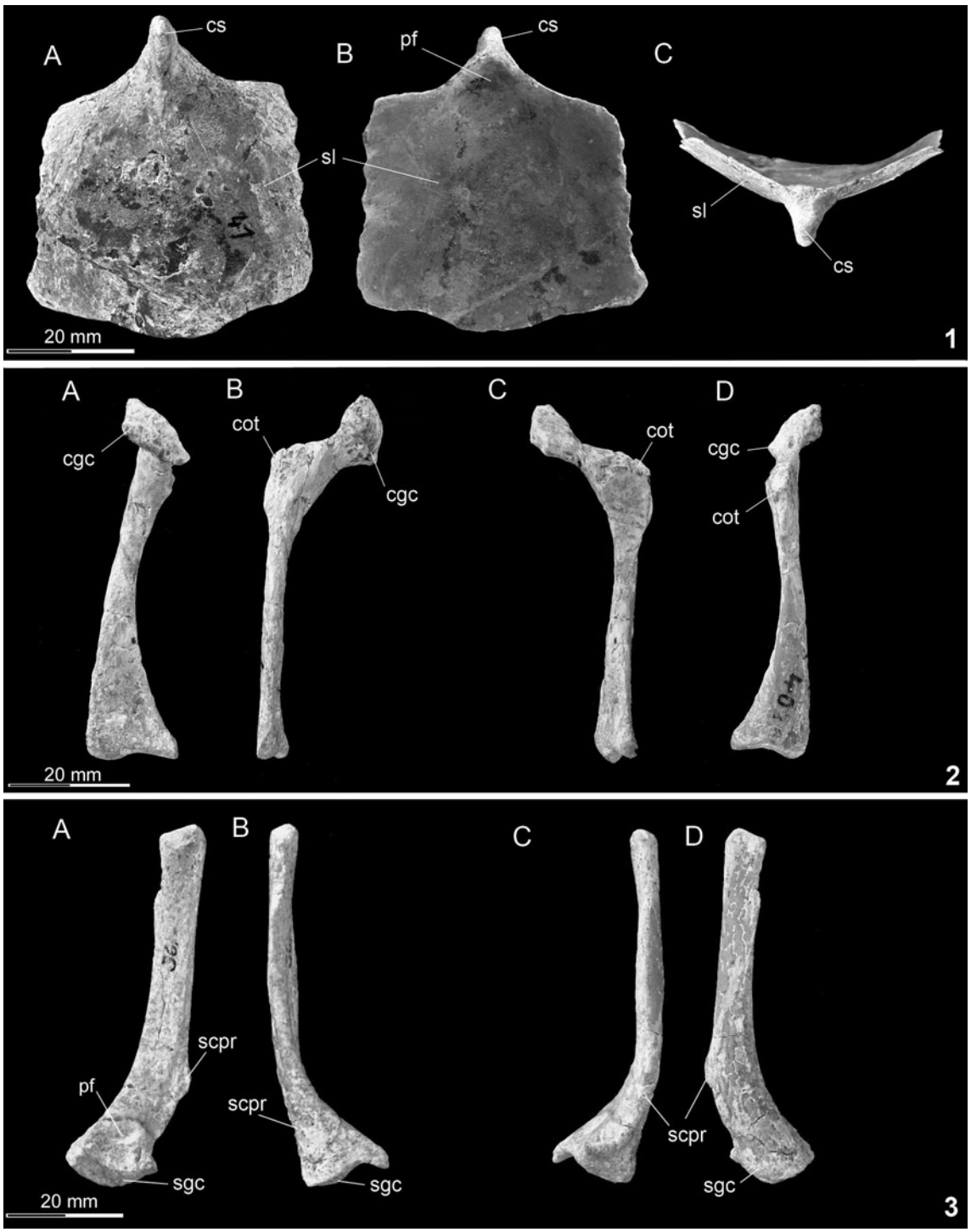

Fig. 6 *Tapejara wellnhoferi*, SMNK PAL 1137: Pectoral girdle. Plate **1**. Sternal plate in ventral (*A*), dorsal (*B*) and anterior view (*C*). Plate **2**. Right coracoid in dorsal (*A*), anterior (*B*), posterior (*C*) and ventral view (*D*). Plate **3**. Right scapula in ventral (*A*), medial (*B*), lateral (*C*) and dorsal view (*D*). *cgc* coracoidal glenoidal cavity, *cot* coracoidal tuberculum, *cs* cristospine, *pf* pneumatic foramen, *scpr* scapular posterior process, *sgc* scapular glenoidal cavitas, *sl* sternal lamina

and the sternocoracoidal articulation. The furca of the articular surface is shallow and widely concave. The majority of the coracoideal body, along with the glenoid fossa, is missing.

Scapula

The scapula is a long, blade-like element, approximately 4.7 times as long as it is wide (Fig. 6; plate 3). The

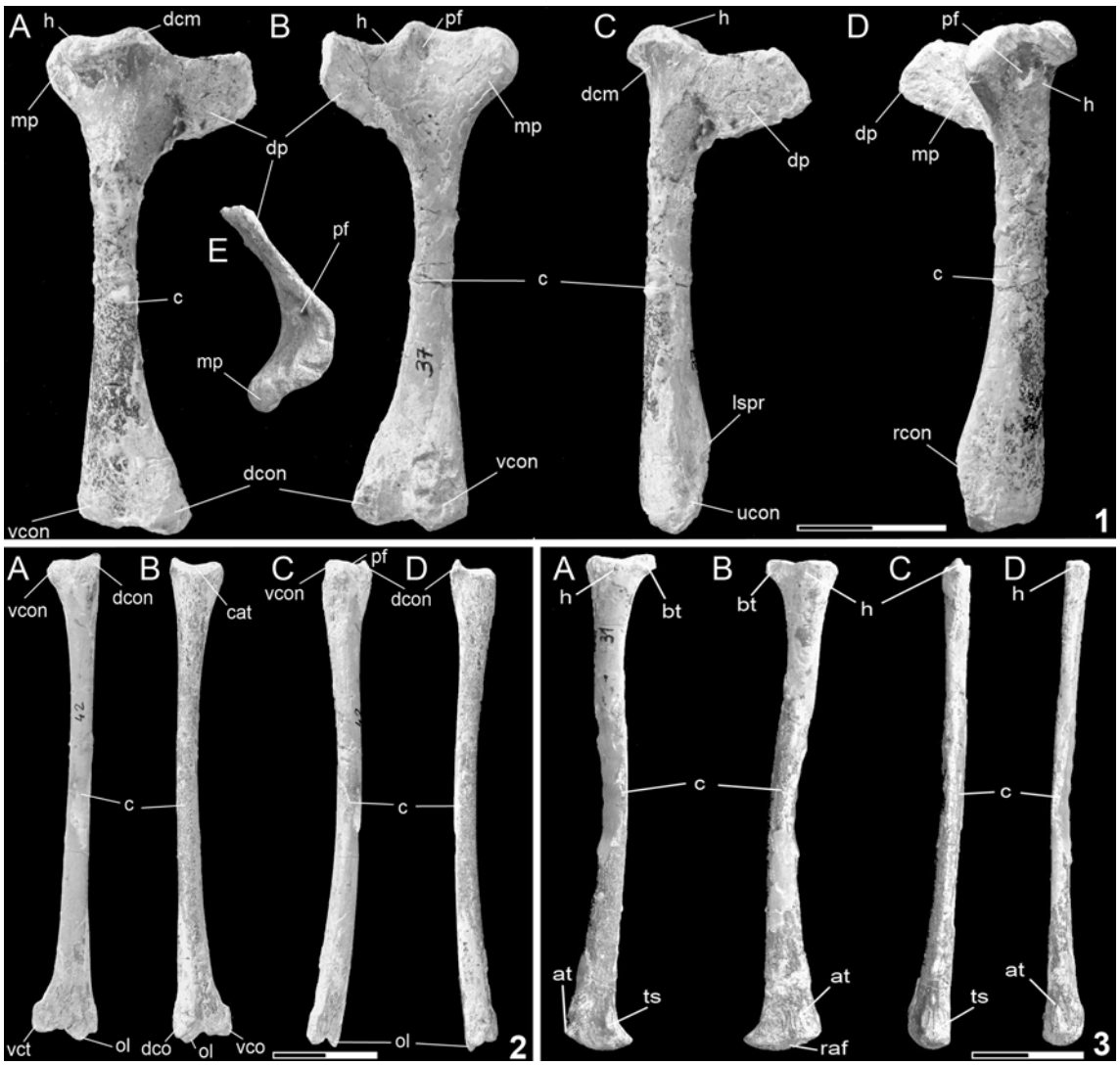

Fig. 7 *Tapejara wellnhoferi*, SMNK PAL 1137: Elements of the forearm I. Plate **1**. Humerus in dorsal (*A*), ventral (*B*), posterior (*C*), anterior (*D*), proximal (*E*) views; Plate **2**. Ulna in anterior (*A*), posterior (*B*), dorsal (*C*), ventral (*D*) aspects; Plate **3**. Radius in anterior (*A*), posterior (*B*), dorsal (*C*), ventral (*D*) aspects. *bt* biccipital tubercle, *c* corpus, *cat* carpal trochlea, *dcm* dorsocranial margin, *dco* dorsal cotyle, *dcon* dorsal condyle, *dp* deltopectoral crest, *h* head (caput), *lspr* lateral supracondylar process, *mp* medial process, *ol* olecranon, *pf* pneumatic foramen, *s* shaft, *ts* tendineous sulcus, *vcon* ventral condyle, *vco* ventral cotyle, *vct* ventral collateral tubercle

proximal third of the scapula is expanded dorsoventrally relative to the remainder of the bone, forming the scapular body and the articular surface with the coracoid. The centre of the articular surface is occupied by a large oval depression. A pronounced anteriorly directed process is positioned on its ventromedial margin. Approximately one third along the length of the scapula a robust tubercle is observed on the lateral margin of the bone, marking the point of transition between the thin scapular blade and body. A single large depression, possibly representing a foramen is observed on the ventral face of the bone, just distal to its proximal termination. The scapular blade itself is curved slightly medially and preserves a more or less constant width along the whole of its length. The medial articular surface shows only a slight dorsoventral expansion relative to the remainder of the blade.

Humerus

The humerus is a long and slender bone, the caput of which is kidney bean shaped and compressed dorsoventrally in its lateral aspect (Fig. 7; plate 1). Relative to the long axis of the shaft the caput is turned strongly dorsally and must have allowed for a large degree of elevation during life. The deltopectoral crest is narrow (1/6th of the total length of the humerus), unwarped and offset at almost 90° to the humeral shaft. In lateral view the deltopectoral crest is regularly curved and directed anteroventrally. The

proximal medial margin preserves a gentle concave curvature that merges with the anterior margin of the caput. The distal margin is damaged. A dorsoventrally compressed process merges with the posterior portion of the caput. Two pneumatopores are observed on the proximal portion of the humerus. The first is located on the ventral face of the collum, between the deltopectoral crest and posterior process (Fig. 7; plate 1B), while the second is located on the dorsal surface of the bone where the posterior process merges with the collum (Fig. 7; plate 1A).

The humeral shaft is mostly straight, circular in cross section, and expands towards its distal terminus to form the articular surface for the radius and ulna. The trochlea and capitulum are widely spaced and separated by a deep intercondylar sulcus that suggests that the humeral epiphyses were not yet sutured with the bone.

Ulna

The ulna is a long, slightly curved bone that preserves an oval cross section between the proximal and distal terminations (Fig. 7; plate 2). The proximal portion has expanded to form a D-shaped articular surface in its proximal aspect, but is badly damaged so that the capitular or trochlear cotyles are only partially observed. Immediately adjacent to the proximal margin a single, possibly pneumatic, foramen is observed on the anterior face of the bone. A long ridge has developed along the ventral half of the bone, presumably for the attachment of antebrachial muscles. As with the proximal articulation the distal portion of the ulna has also expanded dorsoventrally, but is strongly compressed anteroposteriorly. The distal face is poorly preserved.

Radius

The radius is long and very slender but is also badly damaged and missing much of its original compacta. The shaft is slightly anteroposteriorly compressed and is oval in cross section. The proximal and distal portions are expanded to form the respective articular surfaces with the humerus and proximal carpals. A large tubercle process is observed on the dorsoproximal margin of the radius (Fig. 7; plate 3).

Carpals

Five elements of the carpus are preserved, representing two elements of the proximal carpus and two elements of the distal carpus (Fig. 8; plate 1). The carpal elements are poorly preserved but have a complex structure, being typically sub-rectangular in shape with a lot of bony protuberances. Only a single element is recognisable: that of the proximal left anterior carpal, which preserves the concave articular surface for the radius, and a small anterior section of that for the ulna (Fig. 8; plate 1G–J). The two articular depressions are separated by a low ridge. A pronounced tubercle is located on the ventral margin of bone, directly ventral to a large foramen. The absence of the posterior proximal carpal indicates that the formation of a syncarpus had not yet begun.

Metacarpalia I-III

The first three metacarpal bones are very thin but are all incomplete and represented by only small fragments of their distal ends. Here the bone is expanded relative to the shaft and forms a blunt, anteroposteriorly compressed blade that acts as the articular surface of the proximal phalanges of the manual digits I thru III (Fig. 8; plate 2).

Metacarpal IV

The fourth metacarpal is greatly enlarged relative to the first three. It forms an elongate but slender bone, the shaft of which is thickest immediately adjacent to the proximal articular surface (Fig. 8; plate 3). A step-like notch and a medially directed tubercle are observed on the anterodorsal margin of the proximal face of the bone, where they would have slotted into a similar notch between the anterior and dorsal distal carpals, allowing the two bones to rotate against one another to a limited degree. The shaft of the fourth metacarpal displays only a mild curvature and expands distally to form a pair of condyles for articulation with the first phalanx of the wing finger (Fig. 8; plate 3C). The dorsal condyle is slightly larger than that of the ventral one and is directed dorsally at a slight angle to the long axis of the shaft such that the sulcus between the two condyles is directed posterodorsally, causing the wing finger to rise dorsally during flexion. A large pneumatic foramen pierces the bone on its posterior face between the distal condyles (Fig. 8; plate 3C).

Digits I–III

With the exception of the unguals the first phalanx of digit I is the most robust phalangeal element, its shaft narrowing distally before expanding to form a pair of condyles for the ungual articulation (Fig. 9; plate 4A). The condyles are widely spread, creating a large intercondylar sulcus that extends a small way onto the posterior face of the bone. The remaining phalanges are slender with weakly expanded proximal and distal margins and concave and convex articular faces respectively (Fig. 8; plate 4B–C). A single phalanx preserves an unusual morphology where the proximal surface is sub-triangular in profile, the proximodorsal/

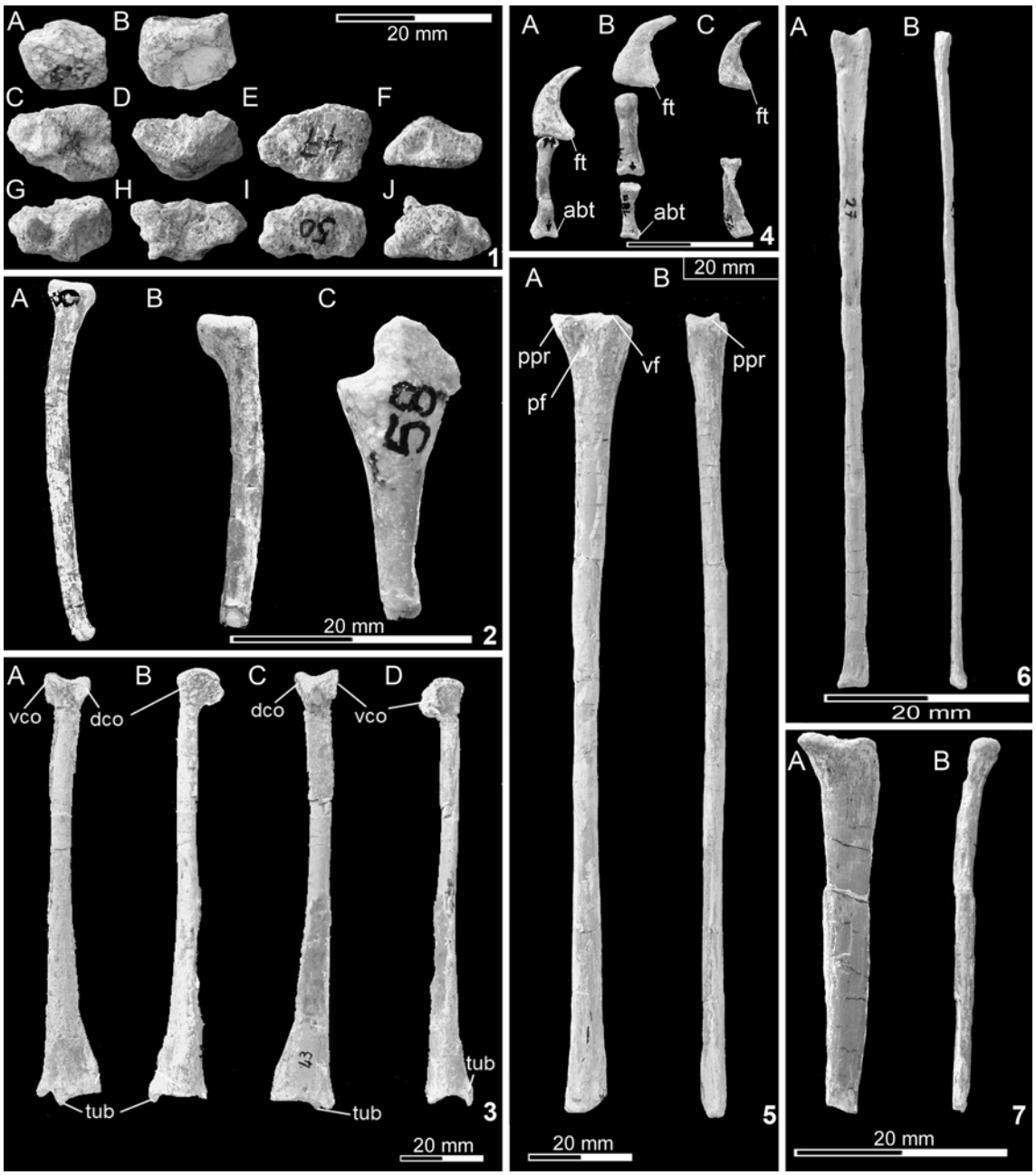

Fig. 8 *Tapejara wellnhoferi*, SMNK PAL 1137: Elements of the forearm II. Plate **1**. Proximal carpals: Preaxial Carpus (*A*, *B*), distal Syncarpus (*C*–*F*), proximal Syncarpus (*G*–*J*); Plate **2**. Metacarpals I–III; Plate **3**. Right metacarpal IV in anterior (*A*), dorsal (*B*), posterior (*C*) and ventral view (*D*). Plate **4**. Digit I–III: Digit I (*A*), Digit II (*B*) and Digit III (*C*). Pate **5**. Digit IV: left wing finger phalanx I in ventral (*A*) and cranial views (*B*). Plate **6**. Digit IV: Right Wing finger phalanx II in ventral (*A*) and cranial view (*B*); Plate **7**. Digit IV: Right Wing finger phalanx IV in ventral (*A*) and anterior view (*B*). *abt* abductor tubercle, *ft* flexor tubercle, *pf* pneumatic foramen, *ppr* posterior process, *vf* ventral fossa

ventral margins of the anterior face being formed by two large tubercles, separated by a pronounced sulcus.

The unguals of the manus are large, robust and more strongly curved than those of the pes. The flexor tubercle is pronounced and occupies approximately one half of the proximal articular surface. A shallow grove extends along the side of some unguals from the proximal margin to the distal tip.

Digit IV—Wing finger phalanges

The elongate first phalanx of the wing finger is a straight element preserving an oval shaped cross section about its mid-shaft (Fig. 8; plate 5). The proximal articular surface is expanded relative to the shaft and is formed by a dorsal and ventral cotyle, the former being approximately twice as

large as the latter and extending in a posterior direction. The extensor tendon process, which forms the anterior halves of the two cotyles is missing, indicating that the two elements had not yet begun to fuse. A large pneumatic foramen is observed on the ventral surface of the bone immediately posterior to the ventral cotyle. While the distal articulation is broken, a slight expansion of the posterior margin of the bone indicates that it is almost complete. The second phalanx is complete but has been badly damaged, requiring the dorsal surface to be coated with an epoxy resin (Fig. 8; plate 6). The bone is straight with an oval cross section, three times as long as high, and is expanded by the proximal and distal margins, forming the articular surfaces. The fourth phalanx is preserved only as a fragment including the proximal articular surface (Fig. 8; plate 7).

Ilium

A partial ilium is preserved from the left hand side of the body, missing only the postacetabular process (Fig. 9; plate 1). The anterior iliac process, forming two third of the total length of the bone, is preserved as an elongate, dorsoventrally compressed blade, the medial and lateral margins of which form a slightly concave arc when viewed in their dorsal aspect. The medially directed curvature of the lateral margin becomes very strong towards the anterior end of the process. An oval depression on the medial margin of the bone, immediately posterior to the iliac process, represents the dorsal half of the acetabulum. The dorsal margin is straight and flat.

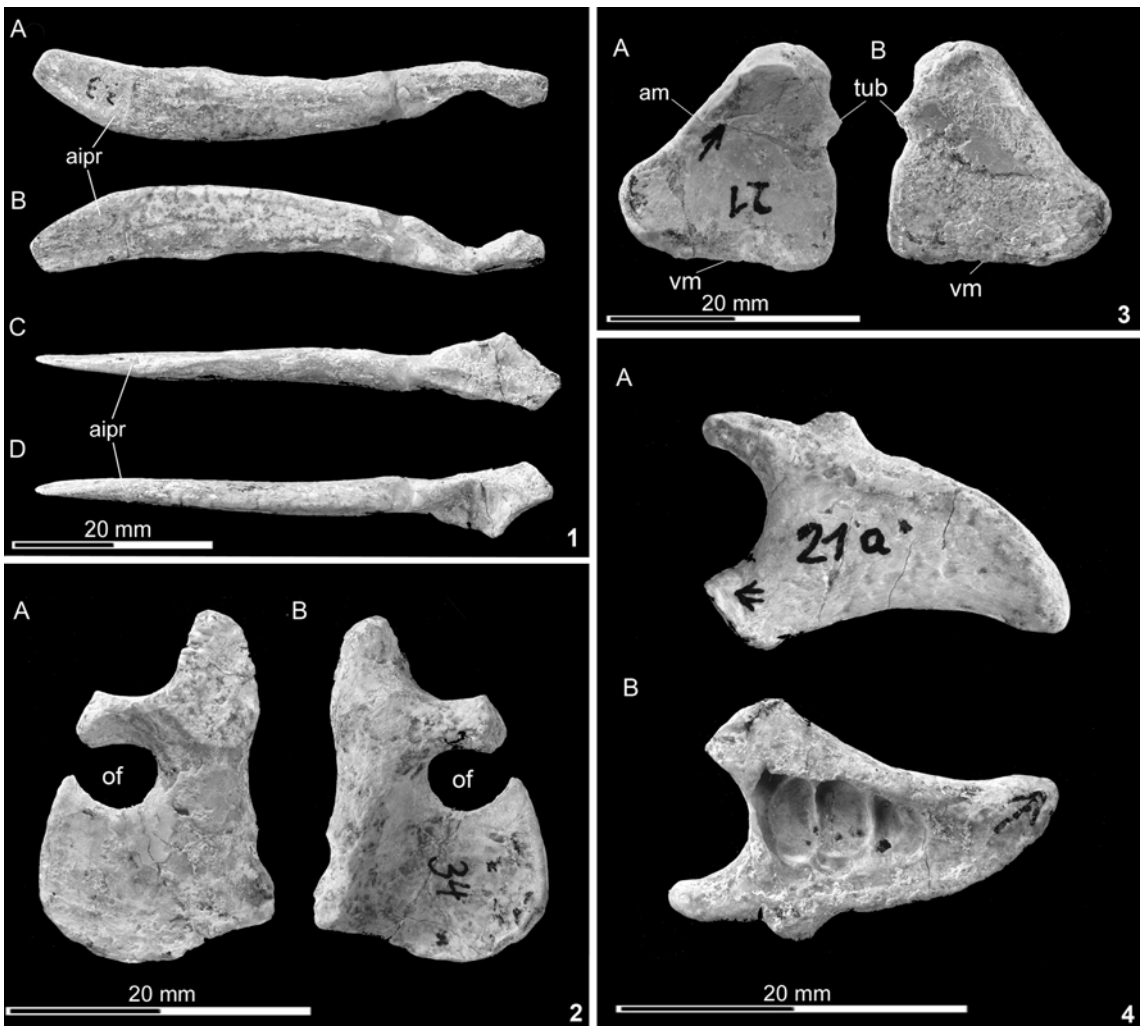

Fig. 9 *Tapejara wellnhoferi*, SMNK PAL 1137: Pelvic girdle. Plate **1**. Left ilium in ventral (*A*), dorsal (*B*), anterior (*C*) and posterior view (*D*); Plate **2**. Left pubis in posterior (*A*) and anterior view (*B*); Plate **3**. Left ischium in medial (*A*) and lateral view (*B*); Plate **4**. Prepubis in dorsal (*A*) and ventral view (*B*). *aipr* anterior iliac process, *am* anterior margin, *of* obturator foramen, *tub* tubercle, *vm* ventral margin

Pubis

The pubis is preserved as a thin isolated plate, the anterior edge of which is straight, forming an angle of just over 90° with the ventral margin (Fig. 9; plate 2). Both the ventral and posterior margins of the bone are convex, with a strongly convex curvature on the posteroventral edge of the pubis. The lateral face is concave. A large sub-circular notch, the obturator foramen, is open via the posterior margin of the bone. Immediately dorsal to the foramen a horizontally orientated, semi-circular bar forms the ventral boundary of the acetabulum. A second bar orientated dorsally and possessing a slightly concave lateral face, marks the anterior and anteroventral margins of the acetabulum.

Ischium

The ischium is a thin, sub-triangular shaped plate of bone, widest along its ventral margin (Fig. 9; plate 3). The anterior margin of the bone is predominantly straight, making an angle of 90° with the ventral margin. A slight concave notch approximately half way down this edge marks the posteriormost portion of the obturator foramen. Immediately dorsal to this the ischiadic expands to form a concave articular face for the horizontal bar of the pubis and defines the posteroventral boundary of the acetabulum.

Prepubis

The prepubis has strongly concave medial and lateral margins, the curvature of the latter being significantly stronger and giving the bone a sub-triangular outline in dorsal view (Fig. 9; plate 4). The proximal articular surface with the pubis is narrow but the bone expands mediolaterally approaching its anterior margin, the edge of which is gently convex but interrupted by a short laterally located tubercle. In ventral view a deep scar for the insertion of abdominal muscles occupies the majority of bone surface.

Femur

Both femora are almost complete, although damage to the bone has removed portions of the caput. The collum is well preserved and is offset against the shaft at an angle of approximately 45° (Fig. 10; plate 1). The fourth trochanter is located lateral to the collum and forms as a prominent triangular process on the dorsal margin of the femur. The lesser trochanter arises from the lateral margin of the greater trochanter. A pneumatic foramen is positioned on the posterior face of the femur between the collum and fourth trochanter. The femoral shaft is straight when viewed from its anterior or posterior aspects but bowed anteriorly in lateral view. The distal articular surface for the tibia is formed by a pair of large condyles, separated by a sulcus that extends for a short distance onto the posterior face of the bone (Fig. 10; plate 1B).

Tibia/Fibula

The right tibia, fibula, tarsals and metatarsals are found in an association with each another and held in position by unprepared sedimentary bridges (Fig. 10; plate 2). The tibia is a narrow and elongate element whose shaft tapers towards the distal termination. The fibular caput contacts the tibia 5 mm distal to the proximal articulation. The fibular shaft lies parallel to the tibia but is broken after a length of 42 mm.

Tarsals

The medial and lateral proximal tarsals are loose elements, separate from the tibia, indicating that a tibiotarsus had not developed. The first tarsal is slightly rhomboid in appearance and divided into two distinct halves by a step-like divide across the centre of the visible face. Sediment cover obscures the remainder of the bone. The second tarsal is sub-rectangular with rounded edges, the dorsal margin being wider than the ventral. The dorsal margin is weakly concave where it would have articulated onto the tibia while the medial face is occupied by a single large depression or foramen. A single rectangular element lies adjacent to the metatarsals and is interpreted as one of the two distal tarsals. Sediment cover prevents any further description.

Metatarsals

All five metatarsals are preserved however the first four are broken after a length of only 11 mm (Fig. 10; plate 2). Metatarsal I–IV are very similar in their cross sectional diameter (1–1.5 mm), with the section itself being either circular, i.e. metatarsals I–II, or oval, metatarsals III–IV. The fifth metatarsal is sub-triangular and very short, with a total length of only 6 mm.

Pes

At least three digits of the pes are present. The phalanges are gracile and display only a mild curvature along their shaft which lies in a natural articulation with the ungual in two of the three elements (Fig. 9; plate 3). The unguals are short and very gracile when compared to those of the manus, but are strongly curved with the ventral margin merging smoothly into the flexor tubercle on the

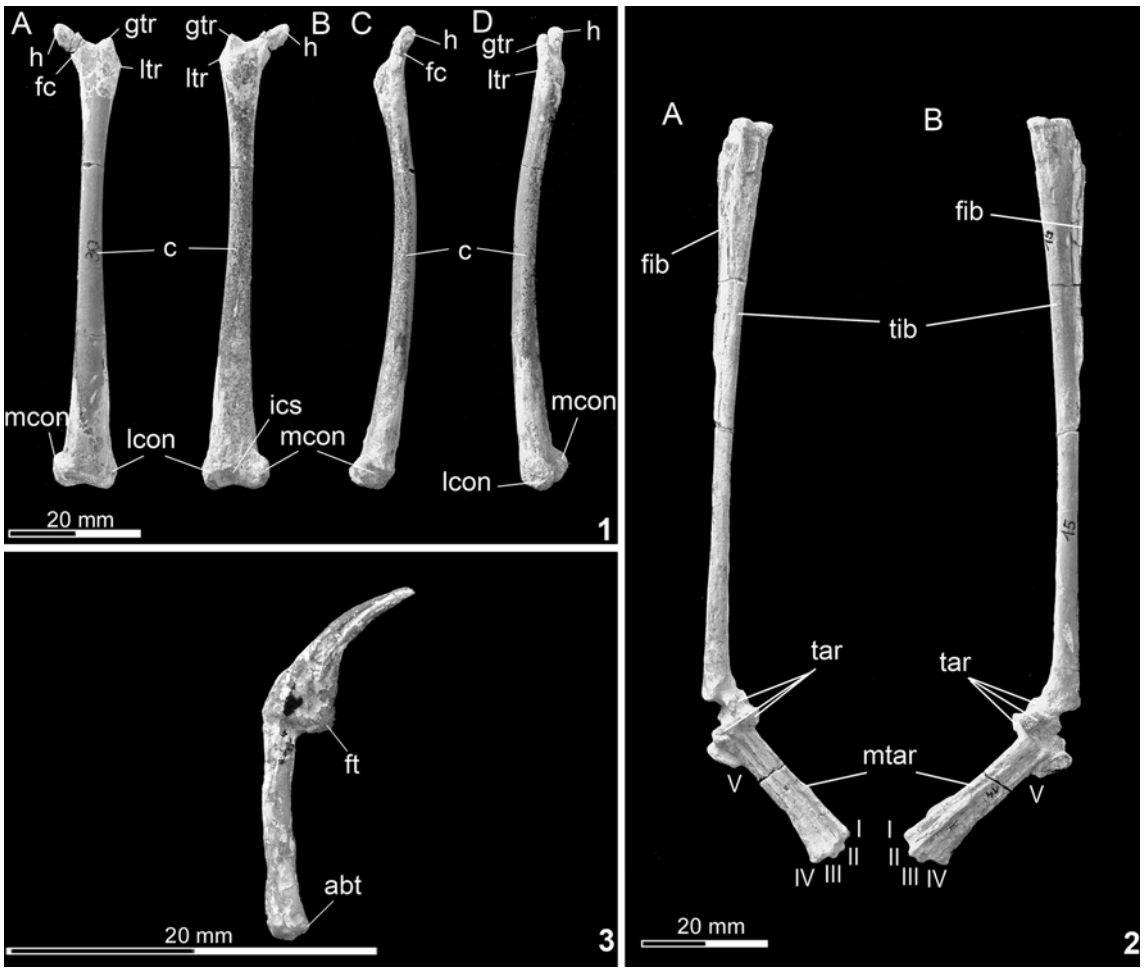

Fig. 10 *Tapejara wellnhoferi*, SMNK PAL 1137: Hindlimb elements. Plate **1**. Left femur in anterior (*A*), posterior (*B*), medial (*C*) and lateral(*D*) views. Plate **2**. Tibia, fibula, tarsals and metatarsals in anterior (*A*) and posterior view (*B*). Plate **3**. Digits of the pes in lateral view. *abt* abductor tubercle, *fc* femoral collum, *fib* fibula, *ft* flexor tubercle, *gtr* greater trochanter, *h* head (caput), *ics* intercondylar sulcus, *lcon* lateral condyle, *ltr* lateral trochanter, *mcon* medial condyle, *mtar* metatarsals, *tar* tarsals, *tib* tibia

proximoventral margin of the bone. A narrow groove extends along the centre of the medial and lateral faces of the bone, terminating just short of the proximal articulation and distal tip.

Discussion

Based on the size difference of the wing metacarpals and the presence of three first wing finger phalanges, two individuals are clearly recognized from the assortment of elements recovered from within the concretion. The larger of these is 1.3 times greater in size than that of the smaller individual which, based on the preserved wing elements, is estimated to have had a wingspan between 1.23 and 1.3 m. The low number of duplicate elements, along with the mostly complete series of neighbouring long bones suggests that the remains are unlikely to represent any additional specimens of a similar size and preservation. The skull is directly associated with the vertebral column through the axis, whose neural canal exactly matches the width of the magnum foramen, inferring that the concretion supported the remains of a single, largely complete individual and the partial wing of another. The presence of both left and right wings for Individual A, along with the coracoid and sternal plate strongly suggests that the skull and majority of the remaining postcranial elements were associated with the smaller of the two animals.

The cranial remains of SMNK PAL 1137 (Fig. 3a) closely match the amended diagnosis for *Tapejara wellnhoferi* (Wellnhofer and Kellner 1991), the presence of a high median crest, short symphysis, mandibular crest and a ventrally turned rostrum, representing several features that distinguish it from other edentulous pterosaurs of the Cretaceous. It is distinct from other taxa of the Tapejaridae (sensu Lü et al. 2006a) by the presence of an elongate parietoccipital process, which renders it distinct from *Tupandactylus navigans* (Frey et al. 2003), while the

nasoantorbital fenestra is reconstructed as being less than twice as high as it is long, with the orbit lying slightly ventral to the level of its dorsal margin. The mandibular crest of SMNK PAL 1137 is less pronounced than that of some specimens of *T. wellnhoferi* (e.g. IMNH 1053 and the reconstructed crest of AMNH 24440), the anterior and posterior margins being more gently concave, however, such a configuration also noted in another specimen also assigned to *T. wellnhoferi* (SMNK PAL 3986). Such a difference in morphology may potentially be regarded as a sexual dimorphism or perhaps, more likely, a factor of ontogenetic maturity where the reconstructed skull length of SMNK 1137 (149 mm from the tip of the beak to the base of the occipital condyle) marks it as the smallest individual that can be confidently assigned to the species. Although Chinese tapejarids also show a less pronounced mandibular crest (i.e. *Sinopterus*, *Huaxiapterus*) the rostrum of these genera is significantly more elongate and slender than that observed in SMNK PAL 1137 and the high dorsally orientated cranial crest differs from the anteriorly directed crest of *Huaxiapterus corollatus* (Lü et al. 2006a) and the low premaxillary crest of *Huaxiapterus jii* (Lü and Yuan 2005). Compared with other skulls of *T. wellnhoferi* (i.e. AMNH 24440) the orbit of SMNK PAL 1137 is located slightly more dorsally (Fig. 3a).

The form of the brain or endocranial cavity is known for *Anhanguera*, *Pterodactylus*, *Dorygnathus*, *Dsungaripterus*, *Pteranodon, Rhamphohynchus* and *Tapejara* (Seeley 1870; Newton 1888; Edinger 1927, 1941; Kellner 1996a, b; Lü et al. 1997, Bennett 2001; Witmer et al. 2003), where it shows a number of similarities to the avian cerebral construction as a presumed consequence of an aerial life. The two very large and transversely convex cerebral lobes that dominate the endocast of SMNK PAL 1137 are very similar in form to that reported in other derived pterodactyloids (i.e. *Anhanguera*, *Pteranodon*), where the individual lobes are only slightly longer than they are broad, but the anterior margins appear less rounded (Fig. 3b, c). Despite a reduced orbit forming part of the diagnosis for *T. wellnhoferi*, the ocular lobes of SMNK PAL 1137 are enlarged relative to those of *Anhanguera* (Witmer et al. 2003), indicating that the animal likely possessed outstanding vision during life. The dorsal surface of the cerebellum is regularly convex until the beginning of the brain stem and more similar to that of *Pteranodon* than the cerebellum of *Anhanguera*, which is more irregular. The enormous floccular lobes reported in other pterosaurian taxa are again observed in *T. wellnhofer* and appear to be completely surrounded by a deep groove that would have accommodated the semi-circular canals. The form of the endocranial cavity in SMNK PAL 1137 thus supports the idea that *Tapejara*, like other pterosaurs for which the brain is known, were competent and very manoeuvrable flyers, relying almost exclusively on visual cues during hunting and social interaction.

A complete comparison of the postcranial elements with other specimens of *T. wellnhoferi* is problematic due to the lack of fossil material, however, a limited comparison is possible with other fossils attributed to the Tapejaridae (sensu Lü et al. 2006a, b), specifically those from China. Although the cervical vertebrae of AMNH 24440 (Wellnhofer and Kellner 1991) are badly broken and do not represent occupy the same position within the cervical series as those presented for SMNK PAL 1137, they nonetheless preserve a similar form with widely diverging prezygapophyses and large foramina flanking the neural canal, but are distinct in that the neural spines appear to be relatively short and low. The length to width ratio of the two midcervicals of SMNK PAL 1137, (i.e. 3 and 3.3) are typical for the low and slightly elongate vertebrae of tapejarid pterosaurs for which a range of 3–4 is known (Lü et al. 2006a).

The rectangular sternal plate of *T. wellnhoferi* is longer than it is wide and has a slightly convex posterior margin, exhibiting an identical form to the tapejarid *Huaxiaopterus jii* (Lü and Yuan 2005) and that of an indeterminate azhdarchoid (MN 6588-V, Sayao and Kellner 2006), where the latter also preserves the costal articulations along the lateral margins of the plate and a relatively short, weakly developed cristospine. While clearly distinct from the ornithocheiroid configuration, for which the length and width of the plate is equal, giving it a D-shaped profile from dorsal view (Kellner and Tomida 2000), the configuration of SMNK PAL 1137 is also more generally applicable to specimens of *Dsungaripterus* and *Pteranodon* (Bennett 2001).

The pectoral girdle of SMNK PAL 1137 is typical of tapejarid pterosaurs where the scapula is slightly longer than the coracoid and gives rise to a "bottom decker" configuration as noted by Frey et al. (2003). The form of the scapula is identical to that observed for Chinese tapejarids where the blade of the element is medially curved and retains an equal width across its length except where it expands to form the coracoid body. The presence or absence of a pronounced tubercle as noted by Kellner (2004) on the posteroventral margin of the coracoid cannot be observed here due to damage to the coracoid body

The humerus is similar in form to other azhdarchoids, where the collum is deflected dorsally at a steep angle and the deltopectoral crest is orientated perpendicular to the long axis of the humeral shaft, the anterior margin of the crest is almost straight. Two foramina are positioned on the dorsal and ventral faces of the proximal humeri respectively, representing a unique configuration to *T. wellnhoferi* (Wang et al. 2009) where the pneumatic system invaded the bone at two locations. This differs from the more basal configuration

observed within the Ornithocheiroidea whereby the pneumatopore is located on the dorsal surface of the bone, where the posterior process meets the collum at the base of the posterior process, and that noted for other azhdarchoids (i.e. *Tupuxuara*, *Quetzalcoatlus*, *Azhdarcho*), where the pneumatic system invades the bone via a large foramen on the ventral face of humeral collum, between the deltopectoral crest and posterior process. Although the position (or presence) of pneumatopores on the humerus is generally unknown in other azhdarchoids, owing to a combination of poor preservation, lateral compression or resting position (e.g. Lü et al. 2006a, ZMNH M8131), Lü et al. (2006b) report that no openings are present on the humerus of the tapejarid *Sinopterus dongi*, indicating that pneumatopore configuration varies within even closely related taxa. This observation suggests that the inclusion of pneumatic features within a generic diagnosis may be warranted. The variability of pneumatopore position further indicates that the observed configurations present throughout the Pterosauria may have evolved multiple times (cf. Classens et al. 2009).

The ulna of *T. wellnhoferi* is identical in form to other azhdarchoids but a pneumatic foramen is situated on the anterior face of the bone immediately adjacent to the proximal articular face. The presence or absence of this feature in other tapejarids is not known, presumably because this section is obscured by the resting position of the fossil, or where crushing has rendered it indistinguishable, but it is observed within two tentative, but undescribed, tapejarids (i.e. SMNK PAL 3985, 3986).

The wing metacarpal is an elongate element relative to the humerus, with that of *T. wellnhoferi* (SMNK PAL 1137) preserving an identical ratio to that of *S. dongi* (i.e. 1.3, Wang and Zhou 2003) but is among the lowest found within the Tapejaridae, the largest of which is observed for *H. benxiensis* (i.e. 2.15). A pneumatopore positioned on the posterior face of the wing metacarpal in SMNK PAL 1137, within the depression reserved for the flexor muscles of the wing finger, represents a feature known only for *Pteranodon* (Bennett 2001). However, this feature in *Pteranodon* is relatively small, whereas for *T. wellnhoferi* it is very large and clearly pierces into the internal cavity.

The first wing finger phalanx is elongate and straight, with a large pneumatopore occupying the ventral face of the bone by the proximal margin, a configuration noted in all pteranodontids, ornithocheiroid and azhdarchoid pterosaurs. Manipulation of this indicates that following the complete flexion of wing phalanges, the pneumatopores of the fourth metacarpal and the first wing finger phalanx close together to form a single, very large pneumatic opening from which both elements are invaded by the diverticulae at a single point on the wing. The first wing finger phalanx of SMNK PAL 1137 makes a ratio of 1.9 with the humerus and agrees very closely with the bivariate ratios known for other tapejarids (i.e., 1.8, *S. dongi*; 2.1–2.8, *Huaxiaopterus*).

The femur is typical of azhdarchoid pterosaurs where a relatively pronounced (for pterosaurs), sub-triangular greater trochanter is present on the dorsal margin of the femur and appears as a partial consequence of an increased terrestrial lifestyle, where a larger attachment area was required for abductor muscles of the femur. The presence of a pneumatic foramen positioned between the greater trochanter and the femoral collum has been noted in *Tupuxuara* and azhdarchid pterosaurs, in addition to a variety of indeterminate azhdarchoids (e.g. SMNK PAL 6409, see Unwin and Martill 2007) but its presence within SMNK PAL 1137 represents its first instance in a specimen that can be confidently assigned to the Tapejaridae. The pneumatic invasion of the hindlimb thus appears to have been widespread, if not universally present, throughout the Azhdarchoidea. Bivariate ratios dictated by the length of the hindlimb within the Tapejaridae indicate that all species show similar, to identical values, where the tibia is 1.39 times longer than the femur in SMNK PAL 1137, and varies between 1.38–1.68 for other tapejarids. The combined length of the hindlimbs to that of the forearm proximal to the wing finger (i.e. humerus, ulna and wing metacarpal) for *T. wellnhoferi* is observed as 1.30 and again agrees very well with other tapejarids (i.e. 1.2, *S.dongi*; 1.2, *H. benxiensis*; 1.36, *H.* jii; 1.4, *H. corollatus*), while that of metatarsal III against the tibia ranges between 0.2–0.24 for *Sinopterus* and *Huaxiapterus*, only slightly lower than that of *T. wellnhoferi* (i.e. 0.28). The similarity of these bivariate ratios between *T. wellnhoferi* and Chinese tapejarids for a variety of long bone elements thus suggests that similar rates of bone development occurred in all tapejarid pterosaurs, although slight differences in ratios noted by Lü et al. (2006b) between specimens of *Sinopterus dongi* indicating that there was a slight variety in intraspecific growth rates, at least for the humerus, femur, mc IV and tibia. Were bones to develop at a significantly different rate between species then they would be clearly manifested given the overall closeness of physical size between individual specimens.

Relative osteological maturity based on the state and sequence of bone sutures known to close throughout ontogeny, confirms that both individuals represented here were morphologically immature and are considered juvenile. Despite the sutures on portions of the skull having already closed, e.g. frontal and parietal, maxilla and premaxilla, complete fusion of the skull was not obtained at the time of death as the quadrate lies separate from the skull. Other elements of the cranial, i.e. jugal, lacrimal, nasal, post orbital are all missing from the concretion suggesting that they had not fused to the preserved portion of the skull. Within the postcranial skeleton the state of the

vertebral column is variable, where the atlas-axis complex is incomplete along with the central bodies of two of the thoracic vertebrae that have not fused to the neural arch. The extensor tendon processes of both Individuals A and B are missing, indicating that they were not fused to the proximal face of the first wing finger phalanx, while the individual elements of the carpus and pelvic girdle remain loose. The tibiotarsus is incomplete, with the proximal tarsals lying separate to the distal articulation, and the scapulocoracoids have not formed. Despite the immature nature of the observed suture states throughout the postcranial skeleton, no pitting or immature bone grain is observed (Bennett 1993).

The observed states of suture closure agrees with that of Kellner and Tomida (2000) and that observed in ornithocheiroid taxa (e.g. NSM-PV 198921; BSP 1982 I 90) where elements of the cranium, principally the premaxillomaxilla, dentaries (forming a symphysis), and frontoparietal fuse very early in ontogeny and prior to other elements of the skull. The timing of suturing in the vertebral column is again similar to that observed in *C. piscator* (NSM-PV 198921) where in both this and the individuals described herein the atlas-axis complex and the posterior cervicals are unfused. These vertebrae are separated by the mid-cervical series in which a mature state, with the suture between the neural arch and centrum fully closed, is observed. Within the thoracic series one anteriorly and one posteriorly located neural arch is lacking the centrum while in the remaining elements the neurocentral suture is completely closed. The described specimens thusly cannot add any support to the idea of a posterior to anterior sequence of suture closure within the vertebral series as is known for crocodilians (Brochu 1996; Kellner and Tomida 2000).

The preservation of multiple carcass assemblages within the fossil record are typically associated with either, sudden and catastrophic events (e.g. sand storms, turbidites, eruptions) or low energy settings that are prone to the collection of transported material (e.g. meander banks of rivers). The association of specimens within the pterosaurian fossil record is rare, and is here reported for the first time in the Santana Formation of NE-Brazil. The large size of the Cretaceous Archipelago, depth of the water bodies between islands, the volant life style of the pterosaurs themselves and the likely long floating periods following their deaths combine to produce a situation where multiple specimens would accumulate in a given locality only under rare circumstances. That one of the specimens described herein is largely complete and contains several small and delicate elements, such as the phalanges of the pes and the metacarpalia, while the other is represented by only portions of the wing, strongly suggests that the animals underwent a varying degree of *post mortem* transportation. Although the similarities in size, ontogenetic maturity and apparent taxonomic status between the two Individuals invite questions as to how they came settle together, the limited amount of locality information, an unfortunate consequence of independent collection, makes it impossible to speculate on these. It must therefore be regarded that the two individuals settled in the same location coincidentally with no further implications, or became entangled during *post mortem* transport.

Conclusions

Two individuals attributed to the Early Cretaceous azhdarchoid *Tapejara wellnhoferi* represent the first instance of two pterosaurian individuals being recovered from a single concretion of the Santana Formation of NE-Brazil. The assorted elements provide the most complete description of postcranial skeleton of *T. wellnhoferi* which although similar to that of other azhdarchoids is distinct in preserving a configuration where the humerus is invaded on both the dorsal and ventral faces of the caput. While this has been previously noted by several studies (Wang et al. 2009) the presence of this feature within a further specimen of *T. wellnhoferi* indicates that intraspecific variation of these characters is unlikely and that owing to the lack of pneumatopores within other members of the Tapejaridae, pneumatic characters may form a useful part of the species diagnosis. The extent of the entire postcranial pneumatic system in *T. wellnhoferi*, whereby pneumatic elements are identified following the guidelines of O'Connor (2006), includes the sternal plate, humeri, ulnae, wing metacarpalia, first wing finger phalanges and femora. The amalgamation of the specimens is considered here to be the likely the product of a lucky coincidence and local currents, where the specimens settled either shortly after one another or became entangled prior to sinking. While the presence of two juvenile animals, attributed to the same taxa and very similar in size may perhaps indicate a local nesting area, the preserved remains suggest that one specimen settled relatively quickly after death while the other is represented by only a partial wing, indicating different periods of surface floating and disintegration.

Acknowledgments We extend our thanks to R. Kastner (SMNK) for preparation of the specimen, V. Griener (SMNK) for assistance with the photographs, Dr Mark Witton and an anonymous referee for their many helpful comments and insights.

References

Bennett, S. C. (1993). The ontogeny of *Pteranodon* and other pterosaurs. *Paleobiology, 19*, 92–106.

Bennett, S. C. (2001). The osteology and functional morphology of the late Cretaceous pterosaur *Pteranodon*. *Palaeontographica A, 260*, 1–153.

Brochu, C. A. (1996). Closure of the neurocentral sutures during crocodilian ontogeny: Implications for maturity assessment in fossil archosaurs. *Journal of Vertebrate Paleontology, 16*, 49–62.

Campos, D. A. & Kellner, A. W. A. (1985). Panorama of the flying reptiles study in Brazil and South America (Pterosauria/Pterodactyloidea/Anhangueridae). *Anais da Academia Brasileira de Ciências, 57*(4):141–142 & 453–466.

Classens, L. P. A. M., O'Connor, P. M., & Unwin, D. M. (2009). Respiratory evolution facilitated the origin of pterosaur flight and aerial gigantism. *PLoS ONE, 4*, e4497. doi: 10.1371/journal.pone.0004497.

Dalla Vecchia, F. M. (1993). *Cearadactylus*? *ligabuei* nov. sp., a new early Cretaceous (Aptian) pterosaur from Chapada do Araripe (Norheastern Brazil). *Bollettino della Società Italiana, 32*(3), 401–409.

De Buisonjé, P. H. (1980). *Santanadactylus brasiliensis* nov. gen., nov. sp., a long-necked, large pterosaurier from the Aptian of Brasil. *Paleontology, Proceedings B, 83*, 158–172.

Edinger, T. (1927). Das Gehirn der Pterosaurier. *Zeitschrift für Anatomie und Entwicklungsgesch, 83*, 106–112.

Edinger, T. (1941). The brain of *Pterodactylus*. *American Journal of Science, 239*, 665–682.

Fastnacht, M. (2001). First record of *Coloborhynchus* (Pterosauria) from the Santana-Formation (Lower Cretaceous) of the Chapada do Araripe, Brazil. *Paläontologische Zeitschrift, 75*, 23–36.

Frey, E., Martill, D. M., & Buchy, M.-C. (2003). A new species of tapejarid pterosaur with soft-tissue head crest. In E. Buffetaut & J.-M. Mazin (Eds.), *Evolution and palaeobiology of pterosaurs* (pp. 65–72). Geological Society of London Special Publications, 217.

Kaup, S. S. (1834). Versuch einer Eintheilung der Saugethiere in 6 Stämme und der Amphibien in 6 Ordnung. *Isis von Oken, 1834*, 311–324.

Kellner, A. W. A. (1984). Ocorrencia de uma mandibula de pterosauria (*Brasileodactylus araripensis,* nov. gen.; nov. sp.) na Formacao Santana, Cretaceo da Chapada do Araripe, Ceara-Brasil. In *Anais XXXIII Cong. Brasil. de Geol.*, Rio de Janeiro, pp. 578–590.

Kellner, A. W. A. (1989). A new edentate pterosaur of the Lower Cretaceous from the Araripe Basin, Northeast Brazil. *Anais de Academia Brasileira de Ciencias, 61*, 439–446.

Kellner, A. W. A. (1996a). *Description of the Braincase of two early cretaceous pterosaurs (Pterodactyloidea) from Brazil*. American Museum of Natural History, New York

Kellner, A. W. A. (1996b). Description of new material of Tapejaridae and Anhangueridae (Pterosauria, Pterodactyloidea) and discussion of Pterosaur phylogeny. Submitted in partial fulfillment of the requirements for the degree of Doctor of Philosophy in the Graduate School of the Arts and Sciences.

Kellner, A. W. A. (2004). New information on the Tapejaraidae (Pterosauria, Pterodactyloidea) and discussion of the relationship of this clade. *Ameghiniana, 41*(4), 521–534.

Kellner, A. W. A., & Campos, D. A. (1994). A new species of *Tupuxuara* (Pterosauria, Tapejaridae) from the Early Creatceous of Brazil. *Anais da Academia Brasileira de Ciências, 66*, 467–473.

Kellner, A. W. A., & Campos, D. A. (2002). The function of the cranial crest and jaws of a unique pterosaur from the early Cretaceous of Brazil. *Science, 297*, 389–392.

Kellner, A. W. A., & Tomida, Y. (2000). Description of new species of Anhangueridae (Pterodactyloidea) with comments on the pterosaur fauna from the Santana-Formation (Aptian-Albian), Northeastern Brazil. *National Sciences Museum Monographs, 17*, 1–135.

Leonardi, G., & Borgomanero, G. (1985). *Cearadactylus atrox* nov. gen., nov. sp.: Novo Pterosauria (Pterodactyloidea) da Chapada do Araripe, Ceara, Brasil. Resumos dos communicaçoes VIII Congresso bras. *de Paleontologia e Stratigrafia, 27*, 75–80.

Lü, J., Du, X., Zhu, Q., Cheng, X., & Luo, D. (1997). Computed tomography (CT) of braincase of *Dsungaripterus weii* (Pterosauria). *Chinese Science Bulletin, 42*, 1125–1130.

Lü, J., Jin, X., Unwin, D. M., Zhou, L., Azuma, Y., & Ji, Q. (2006a). A new species of *Huaxiapterus* (Pterosauria: Pterodactyloidea) from the lower Cretaceous of Western Liaoning, China with comments on the systematics of Tapejarid pterosaurs. *Acta Geologica Sinica, 80*, 315–326.

Lü, J., Liu, J., Wang, X., Gao, C., Meng, Q., & Ji, Q. (2006b). New Material of Pterosaur *Sinopterus* (Reptilia: Pterosauria) from the Early Cretaceous Jiufotang Formation, Western Liaoning, China. *Acta Geologica Sinica, 80*, 783–789.

Lü, J., & Yuan, C. (2005). New Tapejarid Pterosaur from Western Liaoning, China. *Acta Geologica Sinica, 79*, 453–458.

Maisey, J. G. (1991). *Santana-Fossils: An Iilustrated atlas*. Neptune City: T.F.H. Publications, Inc.

Martill, D. M. (2007). The age of the Cretaceous Santana-Formation fossil konsverat Lagerstätte of NO-Brazil: A historical review and an appraisal of the biochronostratigraphic utility of its palaeobiota. *Cretaceous Research, 28*, 895–920.

Neumann, V. H., and Cabrera, L. 1999. Una nueva propuesta estratigráfica para la tectonosecuencia post-rifte de la cuenca de Araripe, noreste de Brasil. In *Bol. 5th Simpósio Sobre o Cretáceo do Brasil, 1999*. UNESP, Campos de Rio Claro, Sao Paulo, pp. 279–285.

Newton, E. T. (1888). On the skull, brain, and auditory organ of a new species of pterosaurian (*Scaphognathus purdoni*), from the Upper Lias near Whitby, Yorkshire. *Philosophical Transactions of the Royal Society of London (B), 179*, 503–537.

O'Connor, P. M. (2006). Postcranial pneumaticity: An evaluation of soft-tissue influences on the postcranial skeleton and the reconstruction of pulmonary anatomy in archosaurs. *Journal of Morphology, 267*, 1199–1226.

Plieninger, F. (1901). Beiträge zur Kenntnis der Flugsaurier. *Palaeontographica, XLVIII*, 64–90.

Pons, D., Berthou, P. Y., & Campos, D. A. (1990). Quelques observations sur la palynologie de l'Aptien superieur et de l'Albien du Bassin d'Araripe. In D. A. de Campos, M. S. S. Viana, P.M. Brito, & G. Beurlen (Eds.), *Atas do Simpósio Sobre a Bacia do Araripe e Bacias Interiores do Nordeste*, Crato, 14–16 de Junho de 1990, pp. 241–252.

Pons, D., Berthou, P. Y., Melo Filgueira, J. B., & Alcantara Sampaio, J. J. (1996). Palynologie des unités lithostratigraphique ''Fundao'', ''Crato'' et Ipubi (Aptien supérieur à Albien inférieur-moyen, Bassin d'Araripe, NE du Brésil): Enseignements paléoécologiques, stratigraphiques et climatologiques. In S. Jardine, I. Klasz, & J.-P. Debenet (Eds.), *Géologie de l'Afrique et de l'Antique Sud. Compte-Rendu des Colloques de Ge'ologie d'Angers, 16–20 July 1994*, Elf Aquitaine, Pau, Mémoire, Vol. 16, pp. 383–401.

Price, L. I. (1971). *A presença da pterosauria no Cretáceo Inferior de Chapada do Araripe, Brasil*. *Academia Brasileira de Ciências, Anais, 43*(Supplement), 451–461.

Sayao, J. M., & Kellner, A. W. A. (2006). Novo esqueleto parcial de pterossauro (Pterodactyloidea, Tapejaridae) do Membo Crato (Aptiano), Formação Santana, Bacia do Araripe, nordeste do Brasil. *Estudos Geológicos, 16*, 16–40.

Seeley, H. G. (1870). *The Ornithosauria: An elementary study of the bones of Pterodactyles*. Cambridge: Cambridge University Press.

Unwin, D. M. (1988). New pterosaurs from Brazil. *Nature, 332*, 398.

Unwin, D. M. (1992). The phylogeny of the Pterosauria. *Journal of Vertebrate Paleontology, 12*(Supplement to No. 3), 57A.

Unwin, D. M., & MartilL, D. M. (2007). Pterosaurs of the Crato Formation. In D. M. Martill, G. Bechly, & R.F. Loveridge (Eds.), *The Crato Fossil Beds of Brazil* (pp. 475–524). London: Cambridge University Press.

Veldmeijer, A. J. (2003). Preliminary description of a skull and wing of a Brazilian Lower Cretaceous (Santana Formation; Aptian-Albian) pterosaur (Pterodactyloidea) in the collection of the AMNH. *PalArch's Journal of Vertebrate Palaeontology, 0*, 1–13.

Wang, X., Kellner, A. W. A., Jiang, S., & Meng, X. (2009). An unusual long-tailed pterosaur with elongated neck from western Liaoning of China. *Anais da Academia Brasileira de Ciências, 81*, 793–812.

Wang, X., Kellner, A. W. A., Zhou, Z., & Campos, D.-A. (2008). Discovery of a rare arboreal forst-dwelling flying reptile (Pterosauria, Pterodactyloidea) from China. *Proceedings of National Academy of Sciences*. doi:10.1073_pnas.0707728105.

Wang, X., & Zhou, Z. (2003). A new pterosaur (Pterodactyloidea, Tapejaridae) from the Early Cretaceous Jiufotang Formation of western Liaoning, China and its implications for biostratigraphy. *Chinese Science Bulletin, 48*, 16–23.

Wellnhofer, P. (1977). *Araripedactylus dehmi* nov. gen., nov. sp., ein neuer Flugsaurier aus der Unterkreide von Brasilien. Mitteilungen der Bayerische Staatsammlung für Paläontologie und historische. *Geologie, 17*, 157–167.

Wellnhofer, P. (1985). Neue Pterosaurier aus der Santana-Formation (Apt) der Chapada do Araripe, Brasilien. *Palaeontographica (A), 187*, 105–182.

Wellnhofer, P. (1987). New crested pterosaurs from the Lower Cretaceous of Brazil. *Mitteilungen der Bayerischen Staatssammlung für Paläontologie und historische Geologie, 27*, 175–186.

Wellnhofer, P. (1991a). Weitere Pterosaurierfunde aus der Santana-Formation (Apt) der Chapada do Araripe, Brasilien. *Palaeontographica (A), 215*, 43–101.

Wellnhofer, P. (1991b). *The illustrated encyclopedia of pterosaurs*. London: Salamander.

Wellnhofer, P., & Kellner, A. W. A. (1991). The skull of *Tapejara wellnhoferi* Kellner (Reptilia: Pterosauria) from the Lower Cretaceous Santana Formation of the Araripe Basin, Northeastern Brazil. *Mitteilungen der bayrischen Staatssammlung für Paläontologie und Historische Geologie, 31*, 89–106.

Witmer, L. M., Chatterjee, S., Franzosa, J., & Rowe, T. (2003). Neuroanatomy of flying reptiles and implications for flight, posture and behaviour. *Nature, 425*, 950–953.

Witton, M. P. (2009). A new species of *Tupuxuara* (Thalassodromidae, Azhdarchoidea) from the Lower Cretaceous Santana Formation of Brazil, with a note on the nomenclature of Thalassodromidae. *Cretaceous Research, 30*, 1293–1300.